Chapter 6

A Review on Supercritical Fluidization

Youjun Lu, Liping Wei and Jikai Huang

Additional information is available at the end of the chapter

http://dx.doi.org/10.5772/intechopen.68180

Abstract

Supercritical water fluidized bed (SCWFB) has been used to gasify biomass, coal and solid waste to produce gas fuel. Supercritical carbon dioxide fluidized bed ($SCCO_2FB$) was applied in the coating industry. Both the two fluidized bed treats the supercritical fluids as fluidization medium. The fluidization behaviours of particles in the supercritical fluids are quite important issues for achieving the basic two phase flow pattern. Few research institutions have conducted experimental and numerical investigations on the fluidization in supercritical conditions. The authors try to establish a comprehensive insight of fluid dynamics of the supercritical fluidized bed. For the SCWFB, the fluidization transitions of fixed bed, homogeneous bed expansion and bubbling were demarcated by discrimination number D_n. A flow pattern map of Reynolds number vs. Archimedes number was available for describing the flow patterns and their boundaries of the $SCCO_2FB$. Ergun equation was acceptable for calculating the fixed bed pressure drop for both SCWFB and $SCCO_2FB$. Wei and Lu correlations of the minimum fluidization velocity, minimum bubbling velocity and homogeneous bed expansion rate are suggested to design the SCWFB. Wen and Yu equation of the minimum fluidization velocity, Vogt et al. correlation of the homogeneous bed expansion rate and their method for determining the minimum bubbling velocity, Nakajima et al. equation of transition velocity, and Bi and Fan correlation of turbulent velocity were recommended to calculate $SSCO_2FB$.

Keywords: supercritical fluids, fluidized bed, flow pattern, simulation, experiment

1. Introduction

Supercritical fluidized bed fluidizes solids with supercritical fluids. The supercritical fluids is the fluid phase, and the solid particles including silica sand, biomass, coal or some coating particles are used in specific applications. Normally, supercritical fluidized bed can be divided into two types according the different supercritical fluids: supercritical water (SCW) and supercritical

carbon dioxide ($SCCO_2$). The critical point of SCW and $SCCO_2$ is T_c = 374°C and P_C = 22.1 MPa, and T_c = 31.26°C, P_C = 7.36 MPa, respectively. The properties including density, viscosity, conductivity, and specific heat capacity vary with operating temperature and pressure. The properties of water are calculated by ISAWP-IF97 equations based on the operating temperature and pressure [1]. The drastic and fast variation of property under temperatures near the pseudo-critical temperature greatly affects the multiphase flow and heat transfer processes [2, 3].

1.1. Applications of supercritical fluidized bed

The supercritical water fluidized bed (SCWFB) has been used for gasifying biomass and coal for hydrogen production. The concept of SCWFB reactor was proposed first by Matsumura and Minowa [4]. In 2008, State Key Laboratory of Multiphase Flow in Power Engineering (SKLMF) of Xi'an Jiaotong University developed a SCWFB reactor for hydrogen production by gasifying wet biomass [5]. The reactor could avoid plugging, increase the hydrogen yield and improve gasification efficiency. Then, SKLMF successfully applied the SCW fluidized bed reactor to gasify coal and established pilot plant for gasification of biomass or coal [6]. In addition, the water fluidized bed operating in high pressure and temperature is a promising reactor for other high temperature water reactions to produce gas or liquid fuels.

The $SCCO_2$ is treated as a solvent and fluidization medium in the fluidized bed. Coating some inert substrate or pharmaceutical particle within the supercritical carbon dioxide fluidized bed ($SCCO_2$FB) can help to improve the material performance or control the release processes of the active substance. The $SCCO_2$FB coating processes have many advantages: narrow particle size distribution, simple process step, simple solvents, moderate temperatures, and easily controlling the particle fluidizations. A further advantage is that they offer control over solid state properties, producing either amorphous or crystalline material and sometimes polymorphs [7].

1.2. Challenges of supercritical fluidized bed

One of the challenges for industrial applications of chemical technology of the supercritical fluidized bed is the reliability of continuous running of the reactor. Another challenge of the supercritical fluidized bed is enlargement. The inner diameter or size of the fluidized bed are limited to the operating high temperature and high pressure. An increase in the inner diameter leads to larger wall thickness, which may reduce the heat transfer coefficient. The unclear flow pattern and transitions processes may affect the chemical reaction efficiency. The theories of optimal matching of mass, momentum, heat, and chemical reaction are still not perfect.

1.3. Important issues within the supercritical fluidization

The design and operation of the fluidized bed reactor are greatly dependent on the understanding of the two-phase flow characteristics in the fluidized bed. An exact determination of flow patterns in fluidized bed reactor will help to keep the chemical reaction under suitable conditions. The evolution of flow patterns, key design parameters (minimum fluidization

velocity, minimum bubbling velocity, bed expansion rate, etc.) of the supercritical fluidized bed are important issues for perfecting the theory of the supercritical fluidized bed.

Although the experimental investigations of the supercritical fluidized bed are still limited, the flow patterns and their boundaries of the supercritical fluidized bed have been gradually obtained, and the correlations of the minimum fluidization velocity, homogenous bed expansion rate and minimum bubbling velocity, transition velocity and turbulent velocity were also partially proposed based on the experimental data. They can help readers to understand the basic two-phase flow characteristics and achieve a calculation of design work.

2. Experiment and simulation

2.1. Experiment study

Tarmy et al. [8] studied the three-phase flow characteristics of fluidized beds under a pressure of 17 MPa and temperature of 450°C. Jiang et al. [9] investigated bed contraction and expansion in a gas–liquid–solid fluidized bed at pressures from 0.1 to 17.4 MPa and temperatures from 20 to 94°C. Liu et al. [10] operated a CO_2-fluidized bed system from ambient to 9.4 MPa. The fluidized bed is a stainless steel column with 25 mm i.d. and 1.2 m height. They experimentally studied the fluidization of Geldart Group A, B, and D particles in CO_2 under ambient to supercritical conditions. They found that fluidization of the supercritical CO_2 fluidized bed was intermediate between the classical aggregative (gas-solid system) and particulate (liquid-solid system) fluidizations. Marzocchella and Salatino [11] fluidized Geldart Group A and B particles by CO_2 at temperature of 35°C with pressure ranging from 1 to 8 MPa. The fluidization column consisted of a lower section made of a polycarbonate pipe with height of 600 mm and inner diameter of 30 mm and a higher stainless steel upper section with height of 700 mm. The temperature of CO_2 varies from ambient to 80°C. The pressure varies from ambient to 100 bar and regulated by a back pressure regulating valve. The maximum flow rate was up to 100 kg h^{-1}. Pressure drop transducer and a hot wire anemometer were applied to measure the fluctuations signals, pressure drop, and average voidage. The fluidization regimes of fixed bed, homogeneous bed expansion, bubbling zone, and turbulent regime were mapped. Vogt et al. investigated the fluidization behaviors of supercritical CO_2-fluidized bed with pressure up to 30 MPa [12]. The experimental system was designed with a maximum operating pressure of 35 MPa and a maximum CO_2 flow of 50 kg $\cdot$ h^{-1}. The largest steel autoclave had a volume of 2.5×10^{-3} m^3 with inner diameter of 39 or 21 mm. They provided a comprehensive picture for the supercritical CO_2-fluidized bed when the superficial velocity was not very high. Potic et al. [13] visually studied the fluidization process of Geldart Group A particles in high pressure water within a cylindrical quartz reactor with an internal diameter of 1.0 mm in the range of 0.1–24.4 MPa and 20–500°. Lu et al. [14] experimentally obtained the minimum fluidization velocity by measuring the pressure drops of a SCWFB with a diameter of 35 mm for temperature ranging from 360 to 420°C and pressure ranging from 23 to 27 MPa. Wei and Lu [15] built a SCWFB fluid dynamics teasing systems; the fluidized bed section is made of stainless steel with 1.2 m height and 35 mm inner diameter. It is designed for the temperature up to 550°C and the pressure up to 30 MPa. A porous metal foam with bore diameter of 30 μm

is used as the distributor of the fluidized bed test section, and a metal foam filter is installed in the exit of the fluidized bed to avoid the escape of the bed materials. They measured the fixed bed pressure drop, minimum fluidization velocity, and bed expansion, minimum fluidization bubbling velocity of a water-solid fluidized bed from ambient to supercritical conditions, and they proposed a flow pattern map of the SCWFB.

2.2. Simulation advance

The fluidization of particles in the supercritical fluidized beds has been simulated by few researchers. Potic et al. [13] applied a DPM model to qualitatively simulate a micro-fluidized bed with an inner diameter of 1 mm. The model provided consistent flow structures with the tested results in the sub-critical and supercritical zones. Vogt et al. [16] developed a compromised model to compute the movement of bubbles in a $SCCO_2FB$ on the basis of empirical correlations. The model describes local fluid dynamics within the $SCCO_2FB$ by treating the surrounding emulsion phase as a continuum and bubble as the other phase. Rodriguez-Rojo and Cocero [17] simulated a $SCCO_2FB$ with an Eulerian two-flow model incorporating the classical drag model of Gidaspow. Wei et al. [18] simulated the feeding methods of a SCW fluidized bed reactor based on the Eulerian two-flow model incorporating particle kinetic theory. Bubbling phenomenon of Geldart Group B particles was observed in the simulation results. Lu et al. [19] derived a non-sphere drag equation to determine the momentum transfer between non-sphere particles and fluid in a dilute suspension system. A combination drag of the non-spherical particle drag model and the Ergun equation has been validated by comparing experimental data of the SCWFB. More recently, Lu et al. [20, 21] studied the fluidization process of Geldart Group B particles in SCW by a CFD-DEM model. Fluidization transition of fixed–homogeneous-bubbling zone was observed in the simulation work. The two-fluid model and CFD-DEM model are two effective simulation method to investigate the fluid dynamics of the supercritical fluidized bed.

3. Flow dynamic in the supercritical fluidized bed

Fixed bed pressure drop, minimum fluidization velocity, minimum bubbling velocity, homogeneous expansion rate, bubble properties and transitions, and turbulence flow regimes of the supercritical fluidized bed are summarized. The flow characteristics of each flow regime are analyzed. The correlations for the key parameters are proposed. In this part, the results of measured method or simulated method for obtaining these parameters are discussed. The properties of SCW and $SCCO_2$ used in the experiments were shown in **Tables 1** and **2**, respectively.

P/MPa	27	27	27	27	27	25	23	23
T/°C	201	350	400	430	479	386	421	406
ρ_f/kg.m$-^3$	880.1	616.1	200.0	150.5	108.2	283.8	112.2	136.5
μ_f/10$-^5$ Pa·s	13.5	7.16	3.12	2.96	3.04	3.67	2.71	2.75

Table 1. Properties of SCW.

P/MPa	0.1	2	4	6	8	9.1	10.1	14.8	17.9	24.8
T/°C	18	35	35	35	35	54	57	56	57	57
ρ_f/kg.m^{-3}	1.8	36	85	150	480	266.8	316.4	637.2	707.1	799.1
μ_f/10^{-5}Pa·s	1.46	1.65	1.73	1.91	4.18	2.25	2.49	4.92	5.77	7.13

Table 2. Properties of $SCCO_2$.

3.1. Fixed bed pressure drop

Fixed bed pressure drop is greatly affected by properties of fluid (density and viscosity), solid properties (diameter, density, and shape factor), and superficial velocity and operation conditions. The description of the fixed bed pressure drop is a key element in the calculation of the minimum fluidization velocity. The calculation of fixed bed pressure drop can be achieved by Ergun equation,

$$\frac{\Delta P}{L} = a\frac{(1-\varepsilon)^2}{\varepsilon^3} \times \frac{\mu u}{(\psi d_p)^2} + b\frac{1-\varepsilon}{\varepsilon^3} \times \frac{\rho_f u^2}{\psi d_p} \tag{1}$$

where ΔP is the pressure drop, μ is the viscosity of fluid, ρ_f is the density of fluid, ε is the fixed bed voidage, d_p is the equivalent volume diameter of the particle, and ψ is the sphericity. The parameters a and b are 1.50 and 1.75, respectively, which are from the investigations of Ergun [22]. Ergun equation has been accepted to calculate the fixed bed pressure drop widely in literature [23].

Figure 1(a) shows the bed pressure drop vs. superficial velocity at temperature from ambient to supercritical zone. The pressure drop increased with an increase in the superficial velocity. An elevated temperature greatly affects bed pressure drop, and the main reason is the density and viscosity of high pressure water decrease with an increase in temperature. **Figure 1(b)** shows the simulated instantaneous bed pressure drop under each superficial velocity was time-averaged, and the relationship between bed pressure drop and fluidization number (superficial velocity divided by u_{mf}). When the superficial velocity is below the minimum fluidization velocity u_{mf}, the bed pressure drop increases with the increasing superficial velocity. When the superficial velocity is above the minimum fluidization velocity, the curve of the bed pressure become flat. Wei and Lu [15] found the deviation of Ergun equation was about ±30%, which was suitable for predicating fixed bed pressure drop in the sub-critical and supercritical zones.

Figure 2 shows the pressure drop of $SCCO_2$-fluidized bed. The experimental data are provided by Marzocchella and Salatino [11], and Vogt et al. [12]. It was found that Ergun equation was generally giving a good description of the measured relationship between pressure drop and superficial velocity. Considering the different supercritical fluids and operating pressures and temperature from ambient to supercritical zone, Ergun's equation is also well applicable for fixed bed flow with a supercritical fluid.

3.2. Minimum fluidization velocity

The minimum fluidization velocity serves as a critical parameter for the design and operation of fluidized bed. The determination of minimum fluidization velocity is conventionally based on the

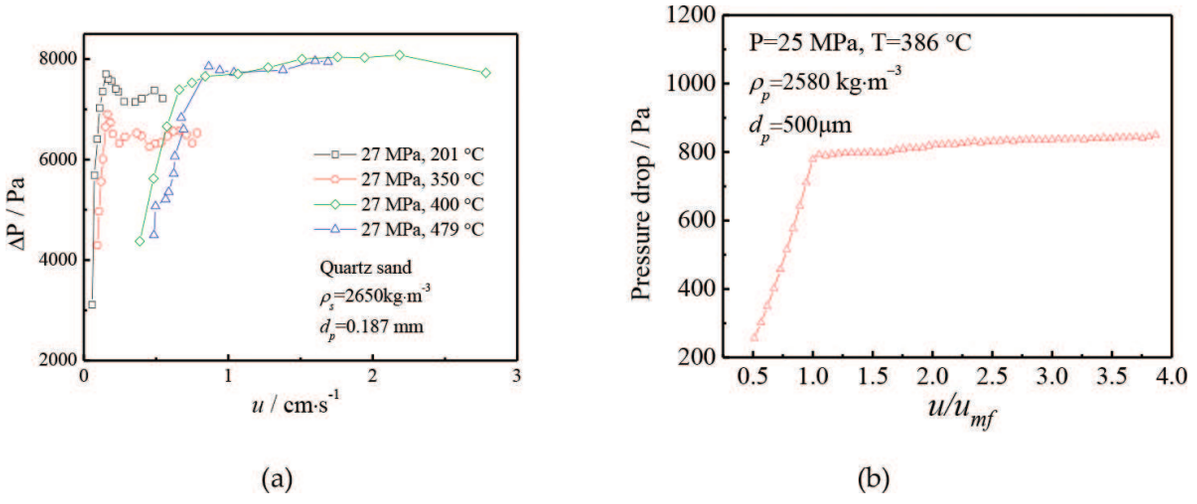

Figure 1. Bed pressure drop vs. superficial velocity for water-solid fluidized bed: (a) experimental data [15] and (b) simulation results by CFD-DEM model [20].

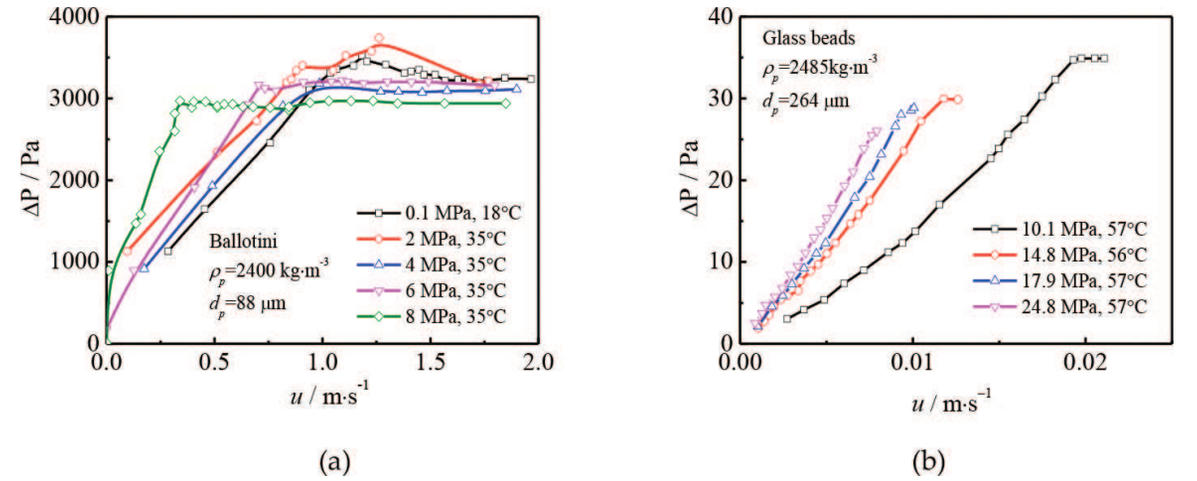

Figure 2. Bed pressure drop vs. superficial velocity for $SCCO_2$ fluidized bed: (a) Marzocchella and Salatino [11], and (b) Vogt et al. [12].

curve of experimentally measured pressure drop vs. superficial velocity. The minimum fluidization velocity was determined by the turning point of the curves, as shown in **Figures 1** and **2**. The minimum fluidization velocity is a function of temperature and pressure for Geldart-A and Geldart-B particles. The minimum fluidization velocity increased with an increase in temperature. The results are attributed to the decrease in density and viscosity of water induces a larger relative velocity for achieving force balance of particles in fluidization. Wei and Lu [15] proposed that an empirical equation of minimum fluidization velocity was achieved for fluidization of Geldart-B and Geldart-A particles in water from ambient zone to supercritical zone. The correlation combined the experimental data in supercritical zone and the expression is shown as follows

$$Re_{\mathrm{mf}} = 6.17\times10^{-4}Ar^{0.9324},\ 70 < Ar < 52000 \tag{2}$$

where Ar is the Archimedes number $Ar = gd_p^3\rho_f(\rho_s - \rho_f)/\mu_f^2$.

In literature, Wen and Yu [24] equation has been usually used to calculate the minimum fluidization velocity of fluidized bed, even at high pressure conditions. Vogt et al. [12] found Wen and Yu equation predicated the minimum fluidization velocity with an average error of 14.3% in a $SCCO_2$ fluidized bed. Rodríguez-Rojo and Cocero [17] also used Wen and Yu equation to determine the minimum fluidization velocity in the simulation work. Marzocchella and Salatino [11] used Chitester et al. [25] equation to calculate the minimum fluidization velocity of the supercritical CO_2 fluidized bed. Wei and Lu [15] have examined the applicability of those reported correlations in SCW fluidized bed. It was found that Wen and Yu equation predicated acceptable minimum fluidization velocity from ambient to supercritical conditions, and the deviations of most predicated results are within ±30%. However, Chitester et al. equation predicated much higher minimum fluidization velocities than the experimental data.

Chitester et al. equation

$$Re_{\mathrm{mf}} = \sqrt{(28.7)^2 + 0.0494Ar} - 28.7 \tag{3}$$

Wen and Yu equation

$$Re_{\mathrm{mf}} = (33.7^2 + 0.0408Ar)^{0.5} - 33.7 \tag{4}$$

3.3. Bed expansion

Figure 3 shows the curves of bed voidage vs. superficial velocity in typical operating conditions for the SCW fluidized bed. The slopes of the curves after the turning point were obviously lower than that before the turning point. Similar phenomena were also observed in the $SCCO_2$ fluidized bed, as shown in **Figure 4**. The turning points of the voidage curves indicated bubbling occurrence in the fluidized bed. The homogenous bed expansion existed before the turning point and after which bubbling was formed. The experimental results show that the transitions from homogenous to bubbling occur in several supercritical conditions for both Geldart A and B particles.

Figure 5 shows the relation curve of bed pressure drop and superficial velocity vs. time. It can be observed that the curve of bed pressure drop vs. time can be divided into three stages.

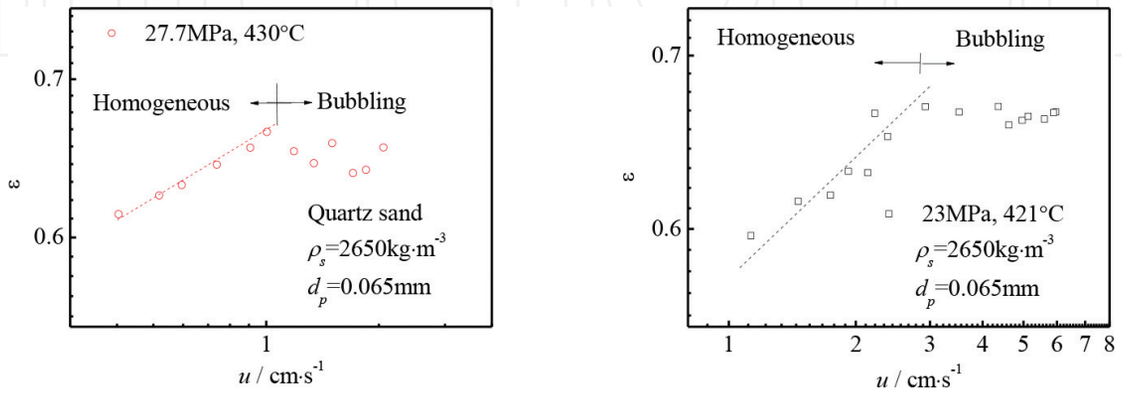

Figure 3. Typical results of voidage vs. superficial velocity for the SCW fluidized bed [20].

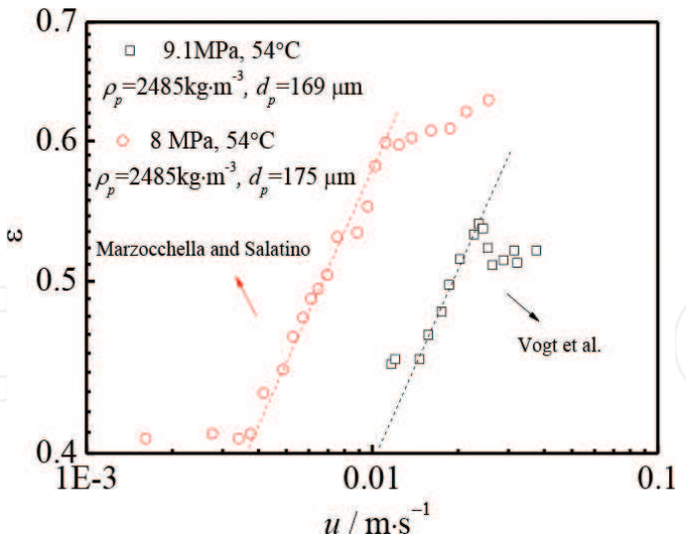

Figure 4. Typical results of voidage vs. superficial velocity for the $SCCO_2$ fluidized bed Vogt et al. [12], and Marzocchella and Salatino [11].

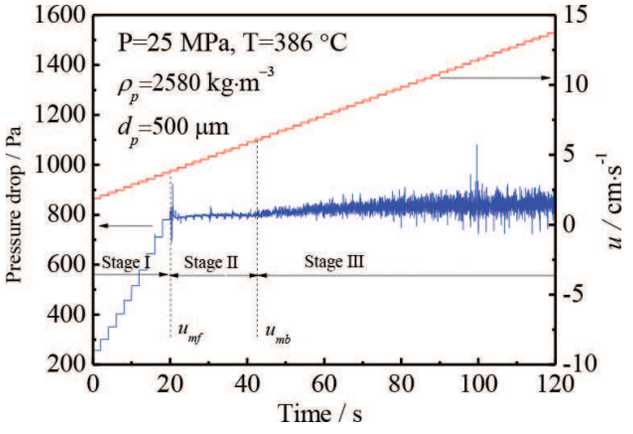

Figure 5. Bed pressure drop and superficial velocity vs. time for the SCW fluidized bed [21].

Stage I, the bed pressure drop increases step by step with the superficial velocity and without fluctuation when $u < u_{mf}$. Stage II, the pressure drop stops increasing with superficial velocity and fluctuates around a fixed value and decays rapidly when $u_{mf} < u < u_{mb}$. Stage III, the pressure fluctuates more violently with the increasing of superficial velocity when $u > u_{mb}$.

Figure 6 shows three snapshots of particles in the three stages. **Figure 6(a)** shows the fixed bed almost no particle moves. **Figure 6(b)** shows the homogeneous fluidization regime without bubbling fluidization in SCW fluidized bed. **Figure 6(c)** shows a bubble fluidization. Bubbles are quite small and scattered in SCW fluidized bed and the bed expansion is more obvious. The distribution characteristics of bubbles benefit the mixing state of fluid phase and solid phase.

For predicating the homogenous bed expansion rate at supercritical pressure, Richardson and Zaki equation [26] was modified based on the experimental data. The basic equation was given:

http://dx.doi.org/10.5772/intechopen.68180

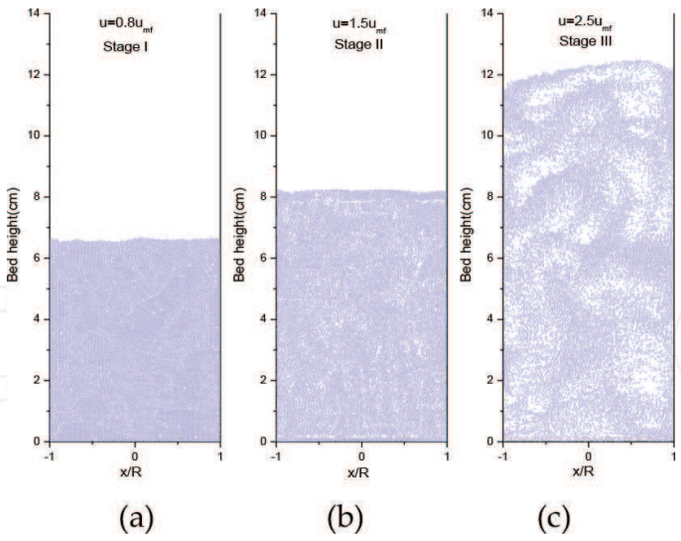

Figure 6. Snapshots of particles in various fluidization regimes [20].

$$u = u_t \varepsilon^n \tag{5}$$

where u_t is the terminal velocity, which can be calculated by correlation from Haider and Levenspiel [27].

Vogt et al. [12] proposed an empirical correlation for homogeneous bed expansion in the $SCCO_2$ fluidized bed, which was given:

$$n = 11.8 Re_t^{-0.23} \tag{6}$$

Wei and Lu [15] provided a modified correlation for homogeneous bed expansion in the SCW fluidized bed, which is shown as follows,

$$n = 10.364 \mathrm{Re}_t^{-0.09973},\ 2 < Re_t < 270 \tag{7}$$

The exponent n obtained from linear fitting of experimental data, thus they diverge each other greatly. The deviation of Eqs. (6) and (7) may indicate that the effects of fluid properties or operating conditions on bed expansion rates are remarkable. Care should be taken to use the bed expansion correlation. The correlation should be carefully used for the design of sub- and supercritical water or $SCCO_2$ fluidized bed.

The Gibilaro's equation [28] was used to predicate the bed expansion of $SCCO_2$ fluidized bed in literature [17].

$$\Delta \mathrm{P} = \left(\frac{18}{Re_p} + 0.33\right) \cdot \frac{\rho_f u^2 H}{d_p} (1 - \varepsilon) \varepsilon^{-4.8} \tag{8}$$

3.4. Bubbling fluidization

3.4.1. Minimum bubbling velocity

The minimum bubble velocity can be obtained from the figure of the standard deviation σ of pressure drop and heat transfer coefficient vs. superficial velocity in the vicinity of the incipient fluidization and incipient bubbling velocities. **Figure 7** shows the simulated and experimentally measured method of the minimum bubbling velocity. As shown in **Figure 7**, before bubbling, the standard deviations kept nearly invariable with an increase in the superficial velocity. After bubbling, an approximately linear relationship between the standard deviation σ and superficial velocity were observed. The onset increase in σ was related to the bubble occurrence. Based on the two methods, the minimum bubbling velocities were obtained.

For the classical gas-solid fluidized bed, Abrahamsen and Geldart correlation is usually used to calculate the minimum bubbling velocity [29]. However, Vogt et al. [12] found Abrahamsen and Geldart correlation predicated a much higher minimum bubbling velocity for the $SCCO_2$ fluidized bed. They suggested to use Foscolo and Gibilaro [30] criterion to predicate the ε_b, and then use Eqs. (5) and (6) to calculate the minimum bubbling velocity by intruding the minimum

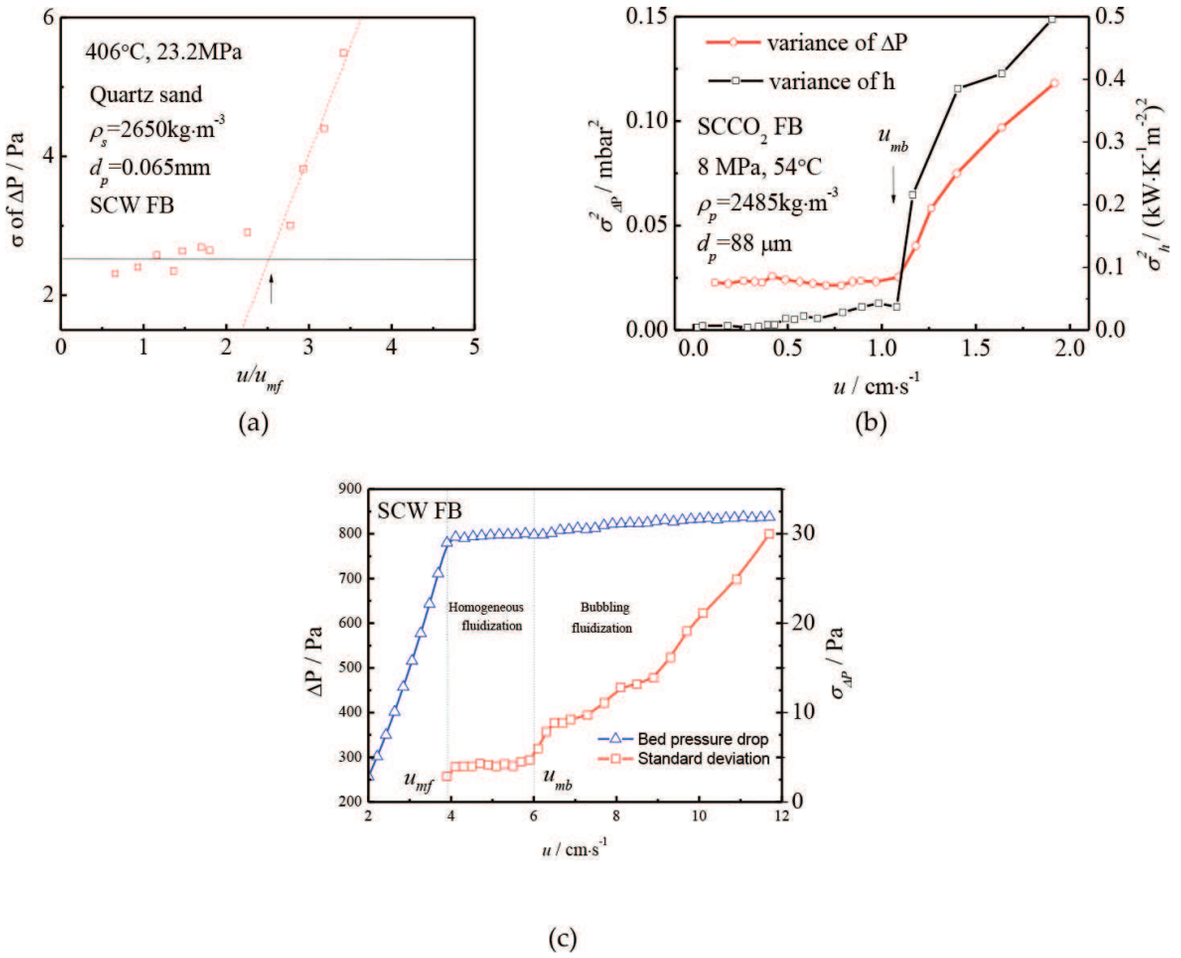

Figure 7. Typical results of variance of variables in the vicinity of incipient fluidization and bubbling: (a) SCW fluidized bed [15], (b) $SCCO_2$ fluidized bed [11], and (c) SCW fluidized bed by CFD-DEM simulation [21].

fluidization velocity and minimum fluidization voidage. Foscolo and Gibilaro found system is homogeneous when the kinematic wave velocity is higher than the dynamic wave velocity, otherwise bubble occurs. When the two velocities are equal, the limit of stability of the system is reached. The criterion is expressed as:

$$\frac{U_d - U_k}{U_k} = \begin{cases} + : \text{Homogeneous} \\ 0 : \text{Stability limit} \\ - : \text{ Bubbling} \end{cases} \tag{9}$$

The kinematic wave speed is

$$U_k = nu_t(1-\varepsilon)\varepsilon^{n-1} \tag{10}$$

The dynamic wave velocity is

$$U_d = \sqrt{3.2gd_p(1-\varepsilon)(\rho_s - \rho_f)/\rho_s} \tag{11}$$

However, Wen and Lu [15] evaluated the adaptability of Foscolo and Gibilaro criterion for the water-solid fluidized bed from ambient to supercritical conditions. They found that Foscolo and Gibilaro's criterion qualitatively predicated bubbling occurrence, the transformation processes of homogenous to bubbling were not captured. Therefore, it was difficult to use Foscolo and Gibilaro's criterion to predicate the minimum bubbling velocity for the SCW fluidized bed. They provided a polynomial function of Archimedes number for calculating the minimum bubbling velocity for the SCWFB.

$$Re_{\text{mb}} = 2\times10^{-8}Ar^2 - 9\times10^{-8}Ar + 1.4608,\ 700 < Ar < 34000 \tag{12}$$

3.4.2. Visible bubble flow rate

Based on the investigations of Vogt et al. [12], the visible bubble flow is multiplying the bubble gas holdup with the local mean bubble rise velocity,

$$V_b = \varepsilon_b u_b \tag{13}$$

The linear relationship between the visible bubble flow and the excess velocity was observed in **Figure 8**.

$$V_b = \phi(u - u_{mb}) \tag{14}$$

where ϕ = 0.6. When the emulsion phase voidage and bed average voidage are known, the bubble voidage can be obtained $\varepsilon_b = (\varepsilon - \varepsilon_e)/(1-\varepsilon_e)$. Then the bubble rising velocity can be calculated by Eq. (13). Eq. 14 reflects a linear relationship between the visible bubble flow and the excess velocity, which is adapted to the ambient conditions. Although the correlation has not been validated for the SCWFB, the equation is suggested to evaluate bubble rising velocity in the situation of lack of reliable formula for predication.

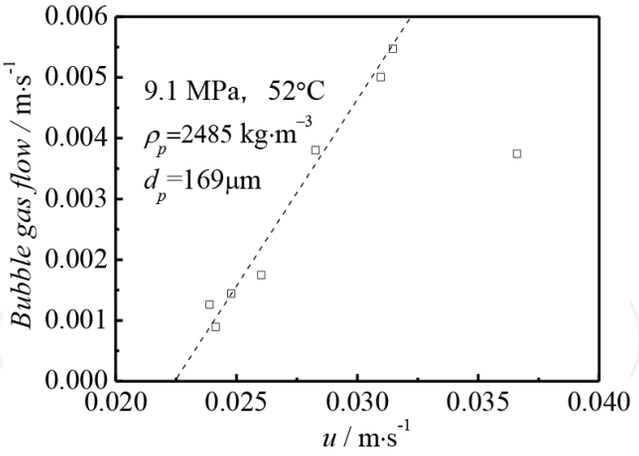

Figure 8. Visible bubble flow for glass beads in the $SCCO_2$ fluidized bed [12].

3.4.3. Effects of fluid states on the bubbling fluidization

Based on the Eulrian two fluid models and non-spherical particle drag model, the fluidized processes of the SCWFB were simulated [19]. **Figure 9** shows the solid distribution of the fluidized bed using different states of water as the fluidization medium and the properties of the SCW were shown in **Table 3**. The superficial velocity was set as 3.5 u_{mf}. **Figure 9(a)–(c)** describes the ambient and sub-critical water-solid system, in which particulate fluidization and homogeneous bed expansion are two typical characteristics. **Figure 9(g)** and **(h)** represents the flow characteristics of the vapor-solid system. **Figure 9(d)–(f)** represents the SCW-solid flow system. In the SCW zone, the pseudo-homogeneous expansion of the bed was similar to the liquid-solid system, but the bubbles occurrence was similar to the gas-solid system. Liu et al. [10] stated that the fluidization in the supercritical CO_2 fluidized bed was an intermediate state between bubbling and homogeneous fluidization through an experimental analysis. The

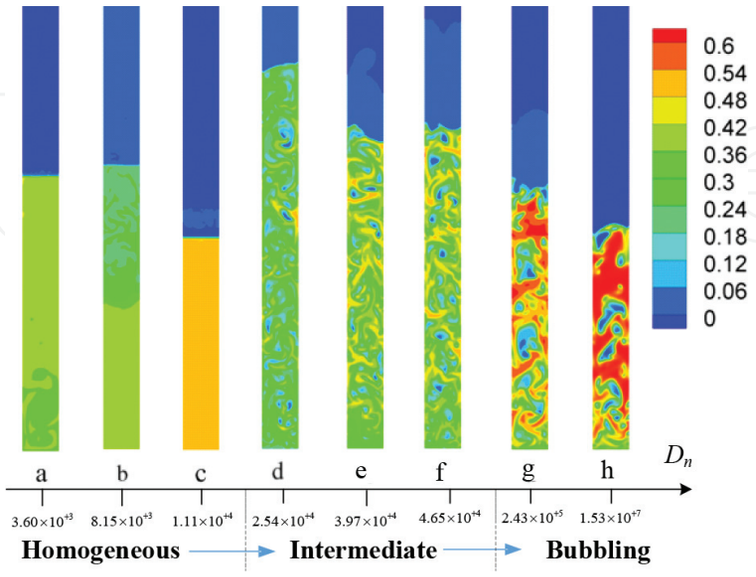

Figure 9. Solid distribution of fluidized bed at different states of water with u / u_{mf} = 3.5 [19].

Fluid states	Ambient	Subcritical		SCW			Steam	
No.	**(a)**	**(b)**	**(c)**	**(d)**	**(e)**	**(f)**	**(g)**	**(h)**
P/MPa	0.1	6.3	25.1	25.4	25.2	25.5	6	0.1
T/°C	20	207	224	387	403	428	400	400
ρ_f/kg.m^{-3}	998.2	859.9	854.1	296.7	162.9	128.7	21.1	0.322
μ_f/10^{-5} Pa·s	100.1	13.06	12.48	3.787	2.913	2.87	2.437	2.446

Table 3. Simulation conditions and parameters in **Figure 9**.

intermediate fluidization has the characteristics of the two-phase flow in both bubbling and homogeneous fluidization. Obviously, the present simulation results showed an intermediate state of the SCW fluidized bed, which was a pseudo-homogeneous expansion with a large number of small bubbles. With an increase in the discrimination number D_n, the fluidization of water-solid system evolved from particulate to intermediate to aggregative.

3.5. Turbulence fluidization and transition zone

Marzocchella and Salatino [11] observed the $\sigma^2_{\Delta P1}/\Delta P_1^2$ vs. u pattern of the $SCCO_2$ fluidized bed is the well-known bell-shaped curve, as shown in **Figure 10**. With an increase in superficial velocity, $\sigma^2_{\Delta P1}/\Delta P_1^2$ increase first and then decrease. Gas superficial velocities at which $\sigma^2_{\Delta P1}/\Delta P_1^2$ is at a maximum and at which it levels off, have been assumed, respectively, as the beginning U_C and the end U_k of the transition to the turbulent fluidization regime. Note that no detectable decrease in the pressure drop across the bed was observed over several minutes of operation of the bed even at fluid superficial velocities over U_k. Based on the experimental investigations, Marzocchella and Salatino [11] suggested Nakajima et al. [31] equation to calculate the transition velocity, and Bi and Fan [32] correlation to determine the turbulent velocity.

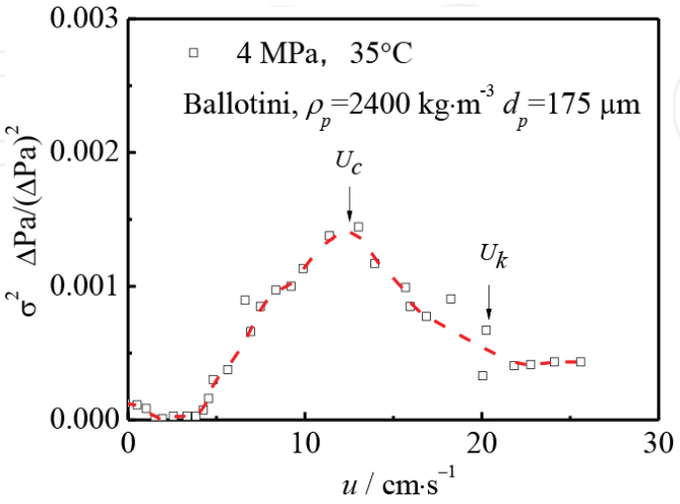

Figure 10. Dimensionless variance of the bed pressure drop vs. superficial fluid velocity for the $SCCO_2$ fluidized bed.

Nakajima et al. equation is,

$$Re_c = 0.663Ar^{0.467} \tag{15}$$

Bi and Fan correlation is,

$$Re_k = \begin{cases} 0.601Ar^{0.695} & Ar \leq 125 \\ 2.28Ar^{0.419} & Ar > 125 \end{cases} \tag{16}$$

4. Flow pattern maps of supercritical fluidized bed

Mapping flow pattern based on experimental data is a useful method to characterize the flow regimes and transitions. For the classical gas-solid or liquid-solid fluidized bed, maps of pressure drop vs. supercritical velocity, slip velocity vs. solid fraction, voidage vs. supercritical velocity, DP standard deviations vs. voidage, non-linear parameters vs. supercritical velocity, dimensionless diameter vs. dimensionless gas velocity, and Reynolds number vs. Archimedes number have been investigated [33, 34, 35]. Those maps can be classified into two groups: dimension and dimensionless. Obviously, the dimensional flow pattern maps are hard to be used in present situation because the fluid state varies greatly from ambient to supercritical conditions. For example, although a plot of velocity vs. fluid density shows a clear physical meaning, it cannot include all the cases for different particles. The dimensionless flow pattern maps are promising to solve the shortcoming. The horizontal ordinates of dimensionless gas velocity or Archimedes number in the traditional flow maps have been proved effective to the classical fluidized bed. However, they are useless for present situations because they cannot discriminate the different transitions of flow regimes. The transitions of flow regimes are mainly depending on the properties of each phases and operating parameters. Obviously, just using Archimedes number cannot reflect effects of both sides. The main obstacle of mapping the flow pattern is describing the horizontal ordinates reasonably.

4.1. SCWFB

Wei and Lu [15] drew the flow pattern maps with abscissa D_n demarcating the three transitions processes and ordinate charactering the operating parameters. The discrimination number D_n was proposed by Liu et al. [10] to demarcate the fluidization quality.

$$D_n = \left(\frac{Ar}{Re_{mf}}\right)\left(\frac{\rho_s - \rho_f}{\rho_f}\right) \tag{17}$$

The discrimination umber shows the effect of properties of two phases in $Ar \cdot \left(\frac{\rho_s - \rho_f}{\rho_f}\right)$, and the effect of operating parameters in $\frac{1}{Re_{\mathrm{mf}}}$. This paper found the discrimination number D_n can demarcate the flow pattern evolution processes. Based on the experimental analysis, fluidization state of fixed-homogeneous (F-H), fixed-homogeneous-bubbling (F-H-B) and fixed-bubbling (F-B) was summarized as follows:

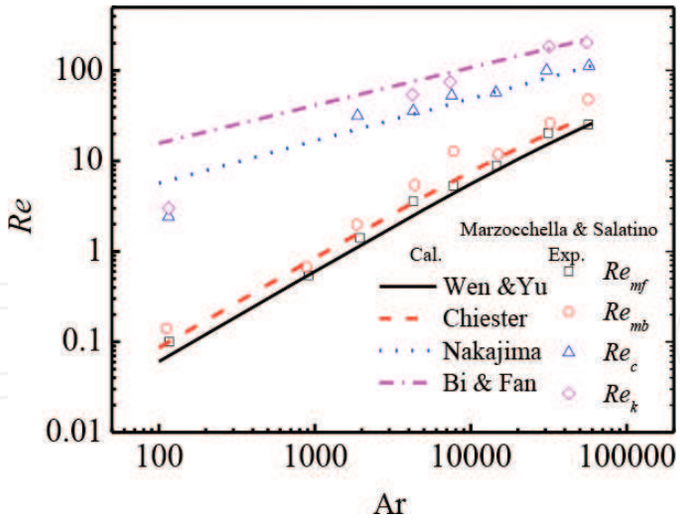

Figure 11. Flow pattern for the $SCCO_2$ fluidized bed.

$$\begin{cases} D_n < 1.2\times10^4 & F-H \\ 1.2\times10^4 \le D_n < 6.4\times10^4 & F-H-B \\ D_n \ge 6.4\times10^4 & F-B \end{cases} \tag{18}$$

The discrimination number D_n of 1.2×10^4 is little higher than the experimental results by Liu et al. [10]. The boundary of F-H fluidization can be determined by the minimum fluidization velocity correlation Eq. (2), and the boundary of F-B and H-B fluidization can be calculated by the minimum bubbling velocity correlation Eq. (12).

4.2. $SSCO_2FB$

Marzocchella and Salatino [11] gave a flow pattern map of Reynolds numbers *Re* vs. Archimedes number for the $SCCO_2$ fluidized bed. In the original map, they calculated Re_{mf} according to Chitester et al. [25] correlation, Re_c by Nakajima et al. [31] correlation, and Re_k could be calculated by Bi and Fan [32]. Here, the map was redrawn by adding the Wen and Yu equation to evaluate the minimum fluidization velocity as shown in **Figure 11**. What's more, the minimum bubble velocity is suggested to be determined according to Foscolo and Gibilaro's criterion.

5. Conclusion

Supercritical bed is a kind of new and promising reactors. This work tries to conduct a comprehensive study on supercritical fluidized bed to provide information of basic two-phase flow and theories of design and operation. A review of main research progress is illustrated and important results were summarized. The main conclusions are obtained as follow:

1. Fixed bed pressure drop in supercritical conditions can be predicated by Ergun equation.
2. Wei and Lu correlation Eq. (2) was suggested as a new correlation for minimum fluidization velocity of water-solid fluidized bed in high pressure, near-critical and supercritical conditions. Wen and Yu equation Eq. (4) was acceptable for calculating the minimum fluidization velocity of the SCWFB and $SCCO_2FB$.
3. The homogeneous bed expansion rate of supercritical fluidized bed can be described by modified Richard and Zaki equation. The index function n can be correlated by Wei and Lu equation Eq. (7) and Vogt et al. equation Eq. (6) for the SCWFB and $SCCO_2FB$, respectively.
4. The bubbling fluidization was found for both Geldart A and B particles in the supercritical fluidized bed. An empirical correlation of minimum bubbling velocity in Eq. (12) was achieved by Wei and Lu for the SCWFB. Vogt et al. provided a method to determine the minimum bubbling velocity of the $SCCO_2FB$ by using Foscolo and Gibilaro criterion.
5. The fluidization state of the supercritical fluidized bed can be viewed as an intermediate between classical gas-solid and liquid-solid fluidizations. The visible bubble flow rate can be predicated by Vogt et al. equation Eq. (14).
6. For the SCWFB, discrimination number D_n was used to determine the fluidization regimes from ambient to supercritical conditions. Fluidization of F-H was found when D_n was below 1.2×10^4; fluidization of F-H-B was found when D_n was between 1.2×10^4 and 6×10^4, and fluidization of F-B was found when D_n was above 6×10^4. As suggested by Marzocchella and Salatino [11], Nakajima et al. [31] equation was used to calculate the transition velocity, and Bi and Fan [32] correlation was applied to determine the turbulent velocity of the $SSCO_2FB$. A flow pattern map of Reynolds numbers Re vs. Archimedes number has been provided for the $SSCO_2FB$.

Acknowledgements

This work is currently supported by the National Natural Science Foundation of China through contract No. 91634109, 51676158, and 51606153.

Nomenclature

Ar	Archimedes number ($Ar = gd_v^3\rho_f(\rho_s - \rho_f)/\mu_f^2$)
d	Particle diameter (m)
d_b	Bubble equivalent diameter (m)
D_n	Discrimination number
FB	Fluidized bed
g	Acceleration due to gravity (m s^{-2})
n	Index function

P	Pressure (Pa)
Re	Reynolds number
Re_p	Particle Reynolds number
Re_t	Terminal Reynolds number
SCW	Supercritical water
$SCCO_2$	Supercritical carbon dioxide
t	Time (s)
T	Temperature (K or °C)
u	Superficial fluid velocity (m s^{-1})
u_{mb}	Minimum bubbling velocity (m s^{-1})
u_{mf}	Minimum fluidization velocity (m s^{-1})
u_t	Terminal velocity (m s^{-1})

Greek letters

ε	Voidage
ρ	Density

Subscripts

c	Transition
f	Fluid
k	Turbulence
o	Initial state
s	Particle phase
t	Terminal state

Author details

Youjun Lu[1]*, Liping Wei[1,2] and Jikai Huang[1]

*Address all correspondence to: yjlu@mail.xjtu.edu.cn

1 State Key Laboratory of Multiphase Flow in Power Engineering (SKLMF), Xi'an Jiaotong University, Xi'an, Shaanxi, China

2 School of Chemical Engineering, Northwest University, Xi'an, Shaanxi, China

References

[1] Wagner W, Kruse A. Properties of water and steam-the industrial standard IAPWS-IF97 for the thermodynamic properties and supplementary equations for other properties: tables based on these equations. Berlin: Springer Verlag; 1998

[2] Wei L, Lu Y, Wei J. Numerical study on laminar free convection heat transfer between sphere particle and high pressure water in pseudo-critical zone. Thermal Science. 2014;**18**(4):1293-1303

[3] Yang CY. Numerical simulation of convection heat transfer for supercritical carbon dioxide in tube. Beijing: North China Electric Power University; 2013

[4] Matsumura Y, Minowa T. Fundamental design of a continuous biomass gasification process using a supercritical water fluidized bed. International Journal of Hydrogen Energy. 2004;**29**(7):701-707

[5] Lu Y, Jin H, Guo L, Zhang X, Cao C, Guo X. Hydrogen production by biomass gasification in supercritical water with a fluidized bed reactor. International Journal of Hydrogen Energy. 2010;**31**(7):822-831

[6] Guo L, Jin H. Boiling coal in water: Hydrogen production and power generation system with zero net CO_2, emission based on coal and supercritical water gasification. International Journal of Hydrogen Energy. 2013;**38**(29):12953-12967

[7] Leeke G A, Lu T, Bridson R H, et al. Application of nano-particle coatings to carrier particles using an integrated fluidized bed supercritical fluid precipitation process. Journal of Supercritical Fluids. 2014;**91**(7):7-14

[8] Tarmy, B, Chang, M, Coulaloglou C, Ponzi, P. Hydrodynamic characteristics of three phase reactors. Chemical Engineer. 1984;**407**:18-23

[9] Jiang P, Luo X, Lin T J, et al. High temperature and high pressure three-phase fluidization—bed expansion phenomena. Powder Technology. 1997;**90**(2):103-113

[10] Liu D, Kwauk M, Li H. Aggregative and particulate fluidization—The two extremes of a continuous spectrum. Chemical Engineering Science. 1996;**51**(17):4045-4063

[11] Marzocchella A, Salatino P. Fluidization of solids with CO_2 at pressures from ambient to supercritical. Aiche Journal. 2000;**46**(5):901-910

[12] Vogt C, Schreiber R, Brunner G, et al. Fluid dynamics of the supercritical fluidized bed. Powder Technology. 2005;**158**(1–3):102-114

[13] Potic B, Kersten S, Ye M, et al. Fluidization with hot compressed water in micro-reactors. Chemical Engineering Science. 2005;**60**(22):5982-5990

[14] Lu Y, Zhao L, Han Q, et al. Minimum fluidization velocities for supercritical water fluidized bed within the range of 633–693K and 23–27MPa. International Journal of Multiphase Flow. 2013;**49**(3):78-82

[15] Wei L, Lu Y. Fluidization behavior in high-pressure water at temperature from ambient to supercritical. Powder Technology. 2016;**304**:89-100

[16] Vogt C, Hartge E, Werther J, et al. Simulation of particle coating in the sueprcrtical fluidized bed. Particuology. 2005;**3**(Z1):113-124

[17] Rodríguez-Rojo S, Cocero M. Supercritical fluidized bed modeling. Journal of Supercritical Fluids. 2009;**50**(1):54-60

[18] Wei L, Lu Y, Wei J. Hydrogen production by supercritical water gasification of biomass: Particle and residence time distribution in fluidized bed reactor. International Journal of Hydrogen Energy. 2013;**38**(29):13117-13124

[19] Lu Y, Wei L, Wei J. A numerical study of bed expansion in supercritical water fluidized bed with a non-spherical particle drag model. Chemical Engineering Research & Design. 2015;**104**:164-173

[20] Lu Y, Huang J, Zheng P. Fluid hydrodynamic characteristics in supercritical water fluidized bed: A DEM simulation study. Chemical Engineering Science. 2014;**117**(1):283-292

[21] Lu Y, Huang J, Zheng P, et al. Flow structure and bubble dynamics in supercritical water fluidized bed and gas fluidized bed: A comparative study. International Journal of Multiphase Flow. 2015;**73**:130-141

[22] Ergun S. Fluid flow through packed columns. Journal of Materials Science & Chemical Engineering. 1952;**48**(2):89-94

[23] Luckos A, Bunt J. Pressure-drop predictions in a fixed-bed coal gasifier. Fuel. 2011;**90**(3): 917-921

[24] Wen C, Yu Y. Mechanics of fluidization. The Chemical Engineering Progress Symposium Series. 1966;**62**:100-111

[25] Chitester D, Kornosky R, Fan L, et al. Characteristics of fluidization at high pressure. Chemical Engineering Science. 1984;**39**(2):253-261

[26] Richardson J, Zaki W. Sedimentation and fluidisation: Part I. Transactions of the Institution of Chemical Engineers. 1954;**32**(35):35-53

[27] Haider A, Levenspiel O. Drag coefficient and terminal velocity of spherical and nonspherical particles. Powder Technology. 1989;**58**(1):63-70

[28] Gibilaro L. Fluidization dynamics. Oxford: Butterworth Heinemann, 2001

[29] Abrahamsen A, Geldart D. Behaviour of gas-fluidized beds of fine powders part I. Homogeneous expansion. Powder Technology. 1980;**26**(1):35-46

[30] Foscolo P, Gibilaro L. A fully predictive criterion for the transition between particulate and aggregate fluidization. Chemical Engineering Science. 1984;**39**(12):1667-1675

[31] Nakajima M, Harada M, Yamazaki R, et al. Bubble fraction and voidage in an emulsion phase in the transition to a turbulent fluidized bed. Kagaku Kogaku Ronbunshu. 1990;**16**(2): 322-328

[32] Bi H, Fan L. Existence of turbulent regime in gas-solid fluidization. Aiche Journal. 1992, **38**(2):297-301

[33] Bi H, Grace J, Zhu J. Regime transitions affecting gas-solids suspensions and fluidized beds. International Journal of Multiphase Flow. 1996;**22**(97):154-161

[34] Bai D, Shibuya E, Nakagawa N, et al. Characterization of gas fluidization regimes using pressure fluctuations. Powder Technology. 1996;**87**(2):105-111

[35] Zhu J, Karamanev D, Bassi A, et al. (Gas-) liquid-solid circulating fluidized beds and their potential applications to bioreactor engineering. Canadian Journal of Chemical Engineering. 2009;**78**(1):82-94

IntechOpen